Available online at www.sciencedirect.com
ScienceDirect
International Journal of Heat and Mass Transfer 50 (2007) 423–432
International Journal of HEAT and MASS TRANSFER
www.elsevier.com/locate/ijhmt

Pool boiling heat transfer on a vertical tube with a partial annulus of closed bottoms

Myeong-Gie Kang

Department of Mechanical Engineering Education, Andong National University, 388 Songchun-dong, Andong-city, Kyungbuk 760-749, South Korea

Received 8 February 2006; received in revised form 27 July 2006
Available online 6 October 2006

Abstract

To improve pool boiling heat transfer in an annulus with closed bottoms, the length of an outer tube has been changed between 0.2 m and 0.6 m. A heated tube of 19.1 mm diameter and the water at atmospheric pressure have been used. Three annular gap sizes of 3.65, 6.35, and 17.95 mm have been investigated. To elucidate effects of the outer tube results of the annulus are compared with the data of a single unrestricted tube. The change in the outer tube length results in much variation in heat transfer. As the outer tube length is much shorter than the heated tube the deterioration point of heat transfer gets moved up to the higher heat fluxes and the possibility of CHF creation is prevented. The major cause of the tendencies is related with the decrease in the intensity of bubble coalescence.

Keywords: Pool boiling; Annulus; Closed bottoms; Vertical tube

1. Introduction

The mechanism of pool boiling heat transfer has been studied extensively in the past since it is closely related with the thermal design of more efficient heat exchangers [1,2]. To have higher heat transfer coefficients is very important if the space for heat exchanger installation is very limited like advanced light water reactors [2,3]. One of the effective means to increase heat transfer is to consider a confined geometry. Major geometries concerning about the crevices are annuli [4–8] and plates [9,10]. Some geometry has closed bottoms [4,6–9]. Some previous studies about the annuli are listed in Table 1.

It is well known from the literature that the confined boiling can result in heat transfer improvement up to 300–800% at low heat fluxes, as compared with unconfined boiling. However, a deterioration of heat transfer appears at higher heat fluxes for confined than for unrestricted boiling [4,6,7]. According to Kang [6], once the flow inlet at the tube bottom is closed, a very rapid increase in the heat transfer coefficient (h_b) is observed at low wall superheat (ΔT_{sat}) less than 2 K. However, increasing ΔT_{sat} more than 2 K the coefficient has almost the same value (i.e. about 20 kW/m^2 K) regardless of the heat flux increase. The cause for the deterioration was suggested as bubble coalescence at the upper regions of the annulus [4]. To adopt the vertical annulus with closed bottoms for the thermal design of a heat exchanger more detailed studies to prevent the deterioration is needed.

Up to the author's knowledge, no previous results concerning the ways have been published yet except the author's preliminary study [8]. Recently, Kang [8] published some results of the vertical annulus (6.35 mm gap) with closed bottoms. To remove the coalescence of the big size bubbles around the upper region of the annulus Kang [8] controlled the length of the outer tube (L_o) of the annulus. The change of the outer length results in much variation in heat transfer coefficients. As the length of the outer tube is much shorter than the length of the heated tube (L) the deterioration point of heat transfer gets moved up to the higher heat fluxes. The reduction of the gap size

E-mail address: mgkang@andong.ac.kr

0017-9310/$ - see front matter © 2006 Elsevier Ltd. All rights reserved.
doi:10.1016/j.ijheatmasstransfer.2006.07.028

Nomenclature

C	parametric constant	q''	heat flux
D	heating tube diameter	s	annular gap size
h_b	boiling heat transfer coefficient	T_{sat}	saturation temperature
I	supplied current	T_W	tube wall temperature
L	heated tube length	t	time
L_o	outer tube length	V	supplied voltage
L_R	ratio of the tubes ($=L_o/L$)	ΔT_{sat}	tube wall superheating ($=T_W - T_{sat}$)

Table 1
Summary of previous works about annular gap effects on pool boiling heat transfer

Author	Remarks
Yao and Chang [4]	– heater: stainless steel tube ($D = 25.4$ mm, $L = 25.4$ and 76.2 mm) – liquid: R-113, acetone, and water at 1 atm – liquid condition: saturated – geometry: vertical annuli with closed bottoms – gap sizes: 0.32, 0.80, and 2.58 mm
Hung and Yao [5]	– heater: stainless steel tube ($D = 25.4$ mm, $L = 101.6$ mm) – liquid: R-113, acetone, and water at 1 atm liquid condition: subcooled or saturated – geometry: horizontal annuli – gap sizes: 0.32, 0.80, and 2.58 mm
Kang [6]	– heater: stainless steel tube ($D = 25.4$ mm, $L = 570$ mm) – liquid: water at 1 atm – liquid condition: saturated – geometry: vertical annuli with open or closed bottoms – gap sizes: 3.9 and 15 mm
Kang and Han [7]	– heater: stainless steel tube ($D = 25.4$ mm, $L = 500$ mm) – liquid: water at 1 atm – liquid condition: saturated – geometry: vertical annuli with open or closed bottoms – gap sizes: 3.9, 15.0, 25.1, 34.9, and 44.3 mm
Kang [8]	– heater: stainless steel tube ($D = 19.1$ mm, $L = 540$ mm) – $L_o = 200$, 400, and 600 mm – liquid: water at 1 atm – liquid condition: saturated – geometry: vertical annuli with closed bottoms – gap sizes: 6.35 mm

(s) also enhances heat transfer [7]. To clarify effects of the outer tube on heat transfer other gap sizes should be studied since the difference in the gap size could results in different tendencies. The present study is to analysis heat transfer in the annulus with closed bottoms through changing the length of the outer tube and the gap size of the annulus.

2. Experiments

A schematic view of the present experimental apparatus and a test section is shown in Fig. 1. The water storage tank (Fig. 1(a)) is made of stainless steel and has a rectangular cross section (950 × 1300 mm) and a height of 1400 mm. The sizes of the inner tank are 800 × 1000 × 1100 mm (depth × width × height). The inside tank has several flow holes (28 mm in diameter) to allow fluid inflow from the outer tank. Four auxiliary heaters (5 kW/heater) were installed at the space between the inside and the outside tank bottoms. The heat exchanger tubes are simulated by a resistance heater (Fig. 1(b)) made of a very smooth stainless steel tube ($L = 0.54$ m and $D = 19.1$ mm). The surface of the tube was finished through buffing process to have smooth surface. Electric power of 220 V AC was supplied through the bottom side of the tube.

The tube outside was instrumented with five T-type sheathed thermocouples (diameter is 1.5 mm). The thermocouple tip (about 10 mm) was bent at a 90° angle and was brazed on the tube wall. The water temperatures were measured with six sheathed T-type thermocouples brazed on a stainless steel tube that placed vertically at a corner of the inside tank. Since the fluid flow is very turbulent the physical mechanism and the temperature reading is not much disturbed by the brazing points. Therefore its effect is neglected. All thermocouples were calibrated at a saturation value (100 °C since all tests were done at atmospheric pressure). To measure and/or control the supplied voltage and current two power supply systems were used. The capacity of each channel is 10 kW.

For the tests, the heat exchanging tube is assembled vertically at the supporter (Fig. 1(a)) and an auxiliary supporter (Fig. 1(c)) is used to fix a glass tube (Fig. 1(c)). To make the annular condition, three glass tubes ($s = 3.65$, 6.35, and 17.95 mm) of different axial length ($L_o = 0.2$, 0.3, 0.4, 0.5, and 0.6 m) were used. A fixture made of slim wires was inserted into the upper side of the gap to keep the space between the heating tubes. The assembled test section is shown in Fig. 1(d).

After the water storage tank is filled with water until the initial water level is reached at 1100 mm, the water is then heated using four pre-heaters at constant power. When the water temperature is reached at a saturation value (i.e., $T_{sat} = 100$ °C since all the tests are run at atmospheric pressure condition), the water is then boiled for 30 min to remove the dissolved air. The temperatures of the tube surface (T_W) are measured when they are at steady state while controlling the heat flux on the tube surface with input

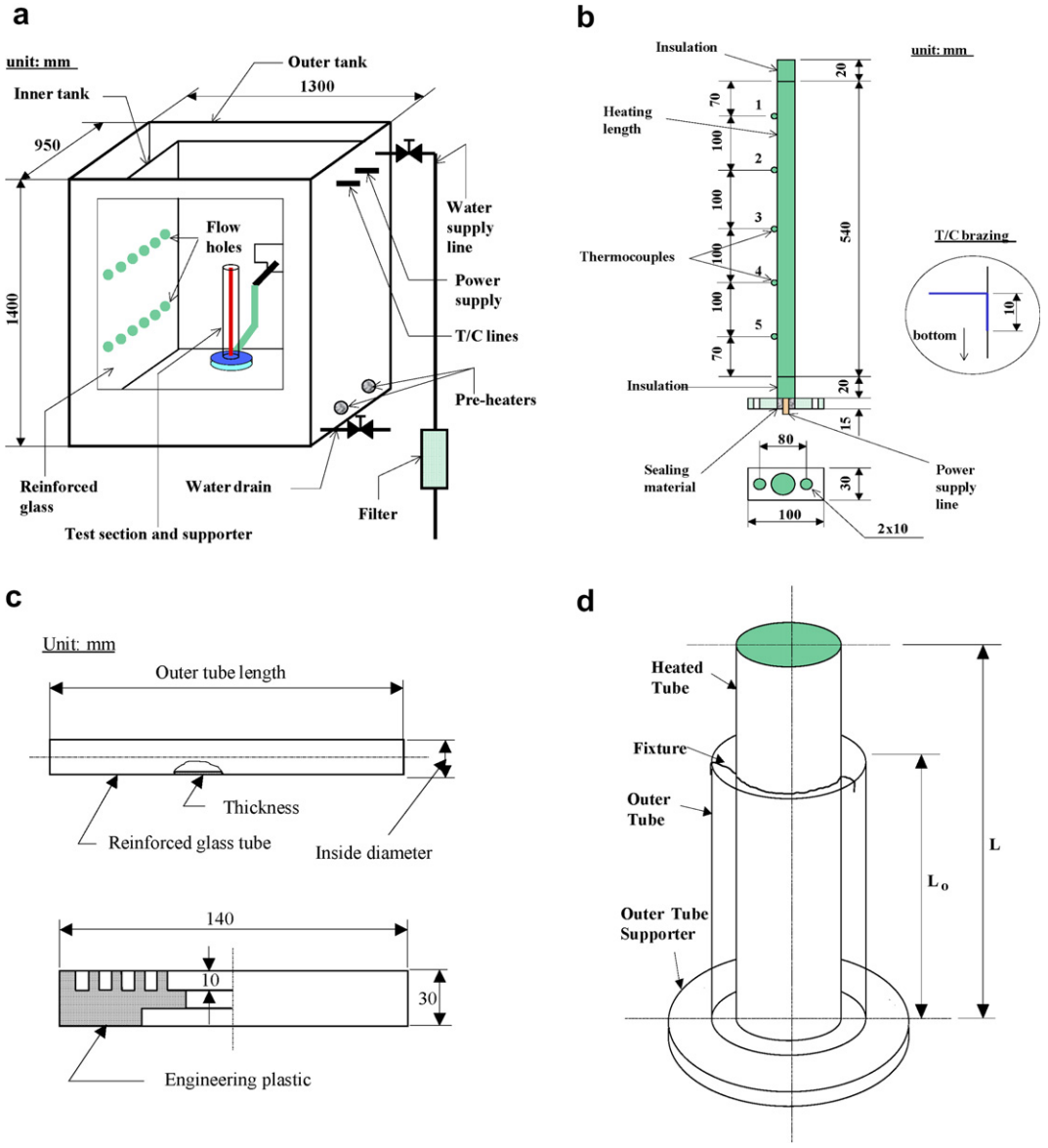

Fig. 1. Schematic diagram of the experimental apparatus.

power. Once a set of experiments has been performed for various heat fluxes, a series of experiments has been executed for the different outer tube length. The single unrestricted tube has been tested at first, and then the annulus is tested.

The heat flux from the electrically heated tube surface is calculated from the measured values of the input power as follows:

$$q'' = \frac{VI}{\pi DL} = h_b \Delta T_{sat} = h_b (T_W - T_{sat}) \quad (1)$$

where V and I are the supplied voltage (in volt) and current (in ampere), and D and L are the outside diameter and the length of the heated tube, respectively. T_W and T_{sat} represent the measured temperatures of the tube surface and the saturated water, respectively. Every temperatures used in Eq. (1) are the arithmetic average values of the temperatures measured by thermocouples.

The error bounds of the voltage and current meters used for the test are ±0.5% of the measured value. Therefore, the calculated power (voltage × current) has ±1.0% error bound. Since the heat flux has the same error bound as the power, the uncertainty in the heat flux is estimated to be ±1.0%. When evaluating the uncertainty of the heat flux, the error of the heat transfer area is not counted since the uncertainties of the tube diameter and the tube length are ±0.1 mm and its effect on the area is negligible.

The measured temperature has uncertainties originated from the thermocouple probe itself, thermocouple brazing, and translation of the measured electric signals to digital values. To evaluate the error bound of a thermocouple probe, three thermocouples brazed on the tube surface

were submerged in an isothermal bath containing water. The measured temperatures were compared with the set temperature (80 °C) of the isothermal bath of ±0.01 K accuracy. Since the duration to finish a set of the present test took less than 1 h, the elapsed time to estimate the uncertainty of the thermocouple probes were set as 1 h. According to the results, the deviation of the measured values from the set value is within ±0.1 K including the accuracy of the isothermal bath. Since the thermocouples were brazed on the tube surface, the conduction error through the brazing metal must be evaluated. The brazing metal is a kind of brass and the averaged brazing thickness is less than 0.1 mm. The maximum temperature decrease due to this brazing is estimated as 0.15 K. To estimate the total uncertainty of the measured temperatures the translation error of the data acquisition system must be included. The error bound of the system is ±0.05 K. Therefore, the total uncertainty of the measured temperatures is defined by adding the above errors and its value is ±0.3 K. The uncertainty in the heat transfer coefficient can be determined through the calculation of $q''/\Delta T_{sat}$ and is within ±10%.

3. Results and discussion

To prove the reproducibility of the experimental data every temperature on the tube surface has been measured twice at the same test condition and the ratios between the first and the second measured values are shown in Fig. 2. The total 899 ratios for the measured local temperatures are within ±1.0% scattering bound throughout the heat fluxes tested. Therefore, it can be said that reproducibility for the tests are obtained throughout this work.

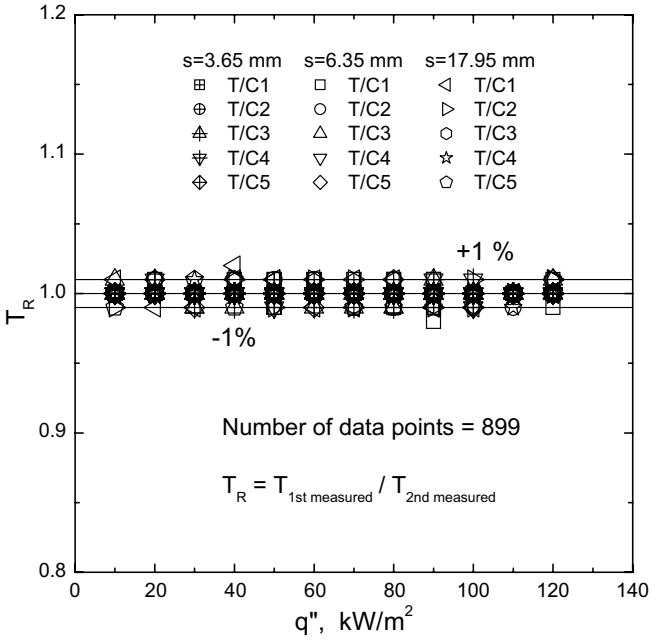

Fig. 2. Reproducibility of the experimental data.

Fig. 3 shows variations in heat transfer as the length of the outer tube and the annular gap size change. To expand Kang's previous study [8], experimental data for $L_o = 0.3$ and 0.5 m are added at $s = 6.35$ mm. Moreover, results of the other two gap sizes (3.65 and 17.95 mm) are newly introduced. Every data for the annuli shows enhanced heat transfer comparing to the unrestricted single tube ($L_o = 0.0$ m). The tube wall superheat for the annuli is much smaller than the single tube at lower heat fluxes. When $s = 3.65$ mm and $q'' = 10$ kW/m^2, ΔT_{sat} for the single tube is about two or three times greater than the annuli depending on the outer tube length. The difference along the tube wall superheats for the annuli and the single tube is increased as the gap size and the heat flux decrease. The major cause of the tendency is because of the active liquid agitation in the annuli. The intensity of liquid agitation in the annuli with closed bottoms is very strong even at lower heat fluxes [6] and the intensity gets stronger as the gap size becomes smaller [7]. In Fig. 3(b) there are some tube wall superheats for the annuli, which are larger than the data for the single tube. The cause is stronger bubble coalescence in the space. The slopes of q'' versus ΔT_{sat} curves are almost same as the gap size is 3.65 or 6.35 mm at $q'' < 60$ kW/m^2. As $s = 17.95$ mm the intensity of liquid agitation is weaker than the other two cases. Therefore, curves of q'' versus ΔT_{sat} have different slopes each other. As the heat flux increases, a kind of deterioration in heat transfer is observed for the annuli. Accordingly, the difference of the tube superheats among the annuli and the single tube gets decreased. The tendency is because of the change in the governing heat transfer mechanism from liquid agitation to bubble coalescence [6]. As shown in the figure the change in L_o results in much variation in heat transfer. However, the tendency strongly depends on the annular gap size. The advantage of adopting the shorter L_o is clearly observed as the annular gap size decreases. In other words, the shortening of L_o gives no improvement in heat transfer comparing to the case of $L_o = 0.6$ m at the wider gap size (see Fig. 3(c)). As the gap size increases deterioration in heat transfer due to the coalesced large bubbles is weak even at higher heat fluxes. As Kang [8] observed already, the deterioration point, where the curve of the annuli cross the curve of the single tube, gets moved up to the higher heat fluxes due to the decrease in L_o from 0.6 m to 0.2 m when the gap size is 6.35 mm. When $s = 3.65$ mm and $L_o = 0.6$ m a sudden initiation of the critical heat flux (CHF) is observed at $q'' = 120$ kW/m^2. For the case of $L_o = 0.6$ m, no significant deterioration in heat transfer is observed at $q'' < 120$ kW/m^2. The deterioration is observed at $L_o = 0.4$ m. This is different from the results of $s = 6.35$ mm. The discrepancy can be explained by the relative intensity of the two competing mechanisms, liquid agitation and bubble coalescence. Since the smaller gap size generates stronger liquid agitation in the annular space [7] and, accordingly, its effect overcomes the deterioration due to the coalesced bubbles, no clear deterioration point is observed in Fig. 3(a) even at $L_o = 0.6$ m. As the length of

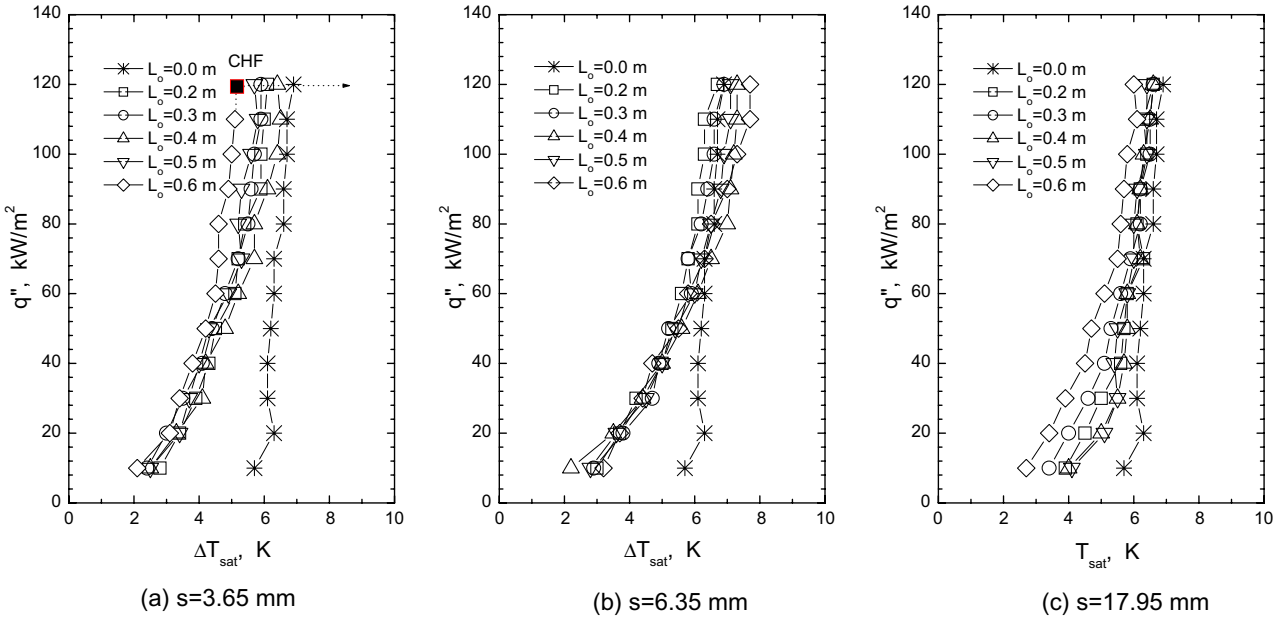

Fig. 3. Curves of q'' versus ΔT_{sat}.

the outer tube gets decreased the intensity of liquid agitation at the upper region of the heated tube decreases and the effect of the coalesced bubbles becomes dominant. As the heat flux increases the incoming liquid interrupts bubbles escaping through the upside of the annulus. Thereafter, bubbles are coalescing in the space and this eventually generates the sudden CHF on the heated tube surface. The local point is around the upper region of the heated tube (i.e., T/C1 location). No CHF is observed as L_o is shorter than 0.6 m. For the gap size of 3.65 or 6.35 mm the decrease of the outer tube length not only moves the deterioration point but also prevents the generation of the CHF. Eventually, it can be concluded that the shortened L_o could solve problems at higher heat fluxes while maintaining the advantages in heat transfer at lower heat fluxes.

Fig. 4 shows some photos of boiling in the annulus ($s = 6.35$ mm) as L_o changes. The closed bottom has restricted net-flow of liquid and the fluid chugging was observed. Those photos were taken at around the mid-point of the tube length. As shown in the photos no active bubble coalescence is observed at $L_o = 0.2$ m. Bubbles coming from the bottom side generates liquid agitation around the upper regions. As the outer tube length increases to 0.4 m tulip type bubbles are observed at the exit. At $t = 2$ s bubble slugs fulfill the exit and prevent liquid inflow to the annular space. At the consecutive time step bubble slugs are moving to the upper regions and, then, relevant liquid inflows to the space. Photos for $L_o = 0.5$ and 0.6 m also show the creation of large coalesced bubbles and the active fluctuation in the annular space.

Variations in heat transfer coefficients due to the changes of L_o and s are shown in Fig. 5. The averaged coefficients along the tube surface are calculated by Eq. (1) and plotted as a function of the heat flux. The increase in the length of the outer tube results in the increase in the discrepancy among the heat transfer coefficients. The difference is magnified as the heat flux increases. However, tendencies of the length effects on the coefficients are not unanimous. Throughout the tube length the narrowest gap size ($s = 3.65$ mm) has the highest heat transfer coefficients for the heat fluxes tested. When the gap size is 6.35 mm the increase of the outer tube length results in a steady decrease in the heat transfer coefficients. At $L_o = 0.4$ m and $q'' \geqslant 60$ kW/m^2 the heat transfer coefficient for the gap size of 17.95 mm is higher than that of 6.35 mm. When the outer tube length is longer than the heated tube length every coefficients for $s = 6.35$ mm is less than the coefficients for $s = 17.95$ mm. The increase in the heat flux and the decrease in the gap size magnify effects of the bubbles on heat transfer. In other words, the higher heat flux generates more bubbles and, then, the narrower gap size accelerates the movement of the bubbles in the space. These bubbles accordingly generate stronger liquid agitation in the annular space. As shown in Fig. 5(c)–(e) a transition point should be exists between two competing heat transfer mechanisms, the bubble coalescence and the liquid agitation. The decrease of the gap size from 17.95 mm to 6.35 mm gradually increases the effect of bubble coalescence on heat transfer. Thereafter, more decrease of the gap size again magnifies the portion of the liquid agitation. This tendency is clearly observed, as the length of the outer tube gets longer than 0.4 m. As $L_o \leqslant 0.4$ m the slopes of the curves for the three gap sizes are almost linear since the effects of the bubble coalescence is hardly observed around the upper region of the heated tube.

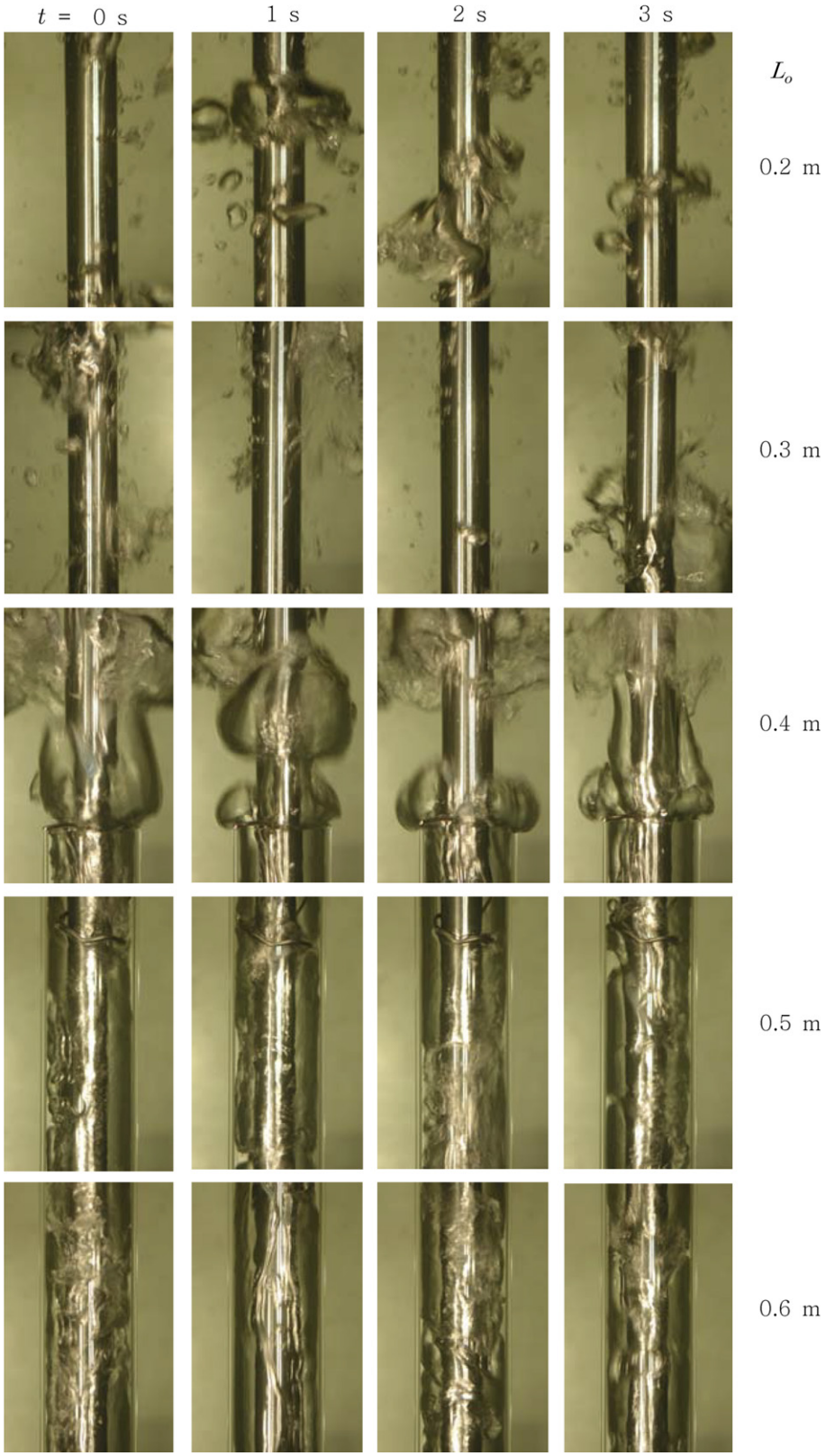

Fig. 4. Photos of boiling on tube surface at $q'' = 30\ \mathrm{kW/m^2}$ for the annulus of $s = 6.35$ mm.

Local heat transfer coefficients at the thermocouple locations are shown in Fig. 6. In the figure ratios of $h_{\mathrm{b,annulus}}/h_{\mathrm{b,single}}$ are shown as the heat flux increases. At T/C1 and $s = 6.35$ mm ratios for $L_{\mathrm{o}} = 0.4$ m has the highest value. At this location no restriction by the outer tube exists for $L_{\mathrm{o}} = 0.4$ m. Thereafter, the stronger liquid agitation overcomes the intensity of the bubble coalescence. However, the other two gap sizes (3.65 and 17.95 mm)

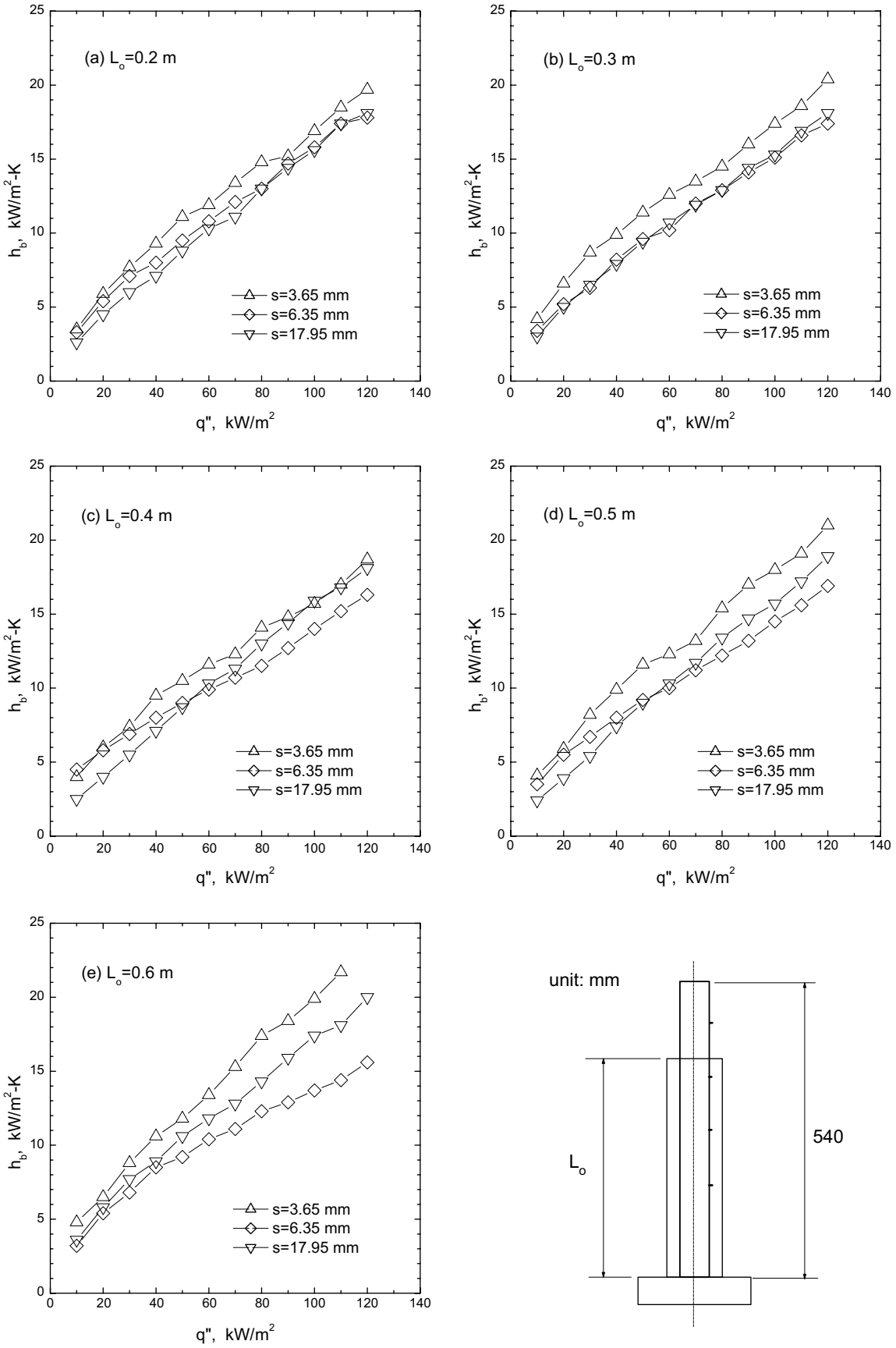

Fig. 5. Variation in heat transfer coefficients as the length of the outer tube and the annular space change.

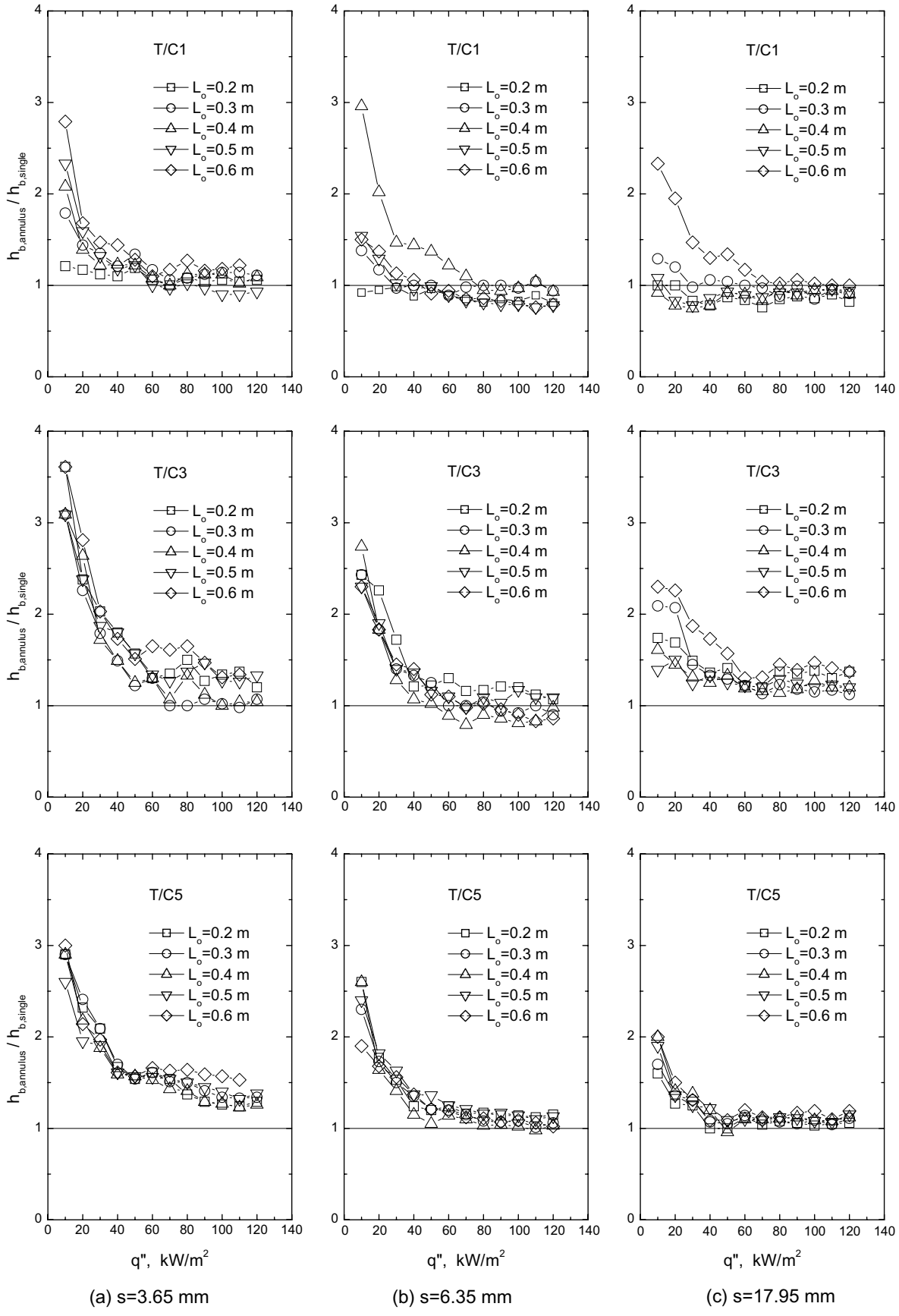

Fig. 6. Comparison of local heat transfer coefficients in the annulus to those of the unrestricted tube.

show different tendency. The highest coefficients are observed at $L_o = 0.6$ m. This means the generation of stronger liquid agitation in the space due to the fluctuation of bubbles. As $L_o = 0.2$ m no enough liquid agitation is shown at this location regardless of the gap size since the bubbles generated at the lower regions are dispersed at this location. For $L_o = 0.6$ m and $s = 6.35$ mm the liquid agitation is activated even at lower heat fluxes and, then, bubble coalescence gets effective as the heat flux increases. As $L_o = 0.2$ m active liquid agitation is observed at T/C3. Local heat transfer coefficients are higher around the locations where changes of the outflow and the inflow are observed. At T/C5 and the gap size is more than 6.35 mm the ratios are nearby 1 as the heat flux is higher than 60 kW/m^2. This means that the existence of the lower liquid agitation at this region. Throughout the tube length, the ratio is larger than 1 (except some data for $L_o = 0.6$ m where bubble coalescence is activated at an early stage) at $q'' < 60$ kW/m^2 where liquid agitation is activated. The ratios are large at T/C5 when the gap size is 3.65 mm. This is because of the active liquid agitation. In a small gap size very active fluctuation of bubbles is observed even at lower heat fluxes. For more clear observation of the outer tube effects on heat transfer the variation in the heat transfer coefficient is shown in Fig. 7 as a function of the dimensionless tube ratio ($L_R = L_o/L$). There is no unanimous tendency. The change in h_b as L_R increases depends on the gap size and the heat flux. At $s = 17.95$ mm and $q'' = 120$ kW/m^2, the increase in L_R results in h_b increase. However, at $s = 6.35$ mm and $q'' = 120$ kW/m^2, the increase in L_R results in h_b decrease.

A total of 179 data points have been obtained for the heat flux versus wall superheat for various combinations of the annular gap and tube length ratios. To take account effects of the gap size, the heat flux, and the tube ratio a simple curve-fitting equation form is considered as follows:

$$h_b = C_1 q''^{C_2} L_R^{C_3} / s^{C_4} \quad (2)$$

In the above equation, the dimensions for h_b, q'', and s are kW/m^2 K, kW/m^2, and mm, respectively. Table 2 lists results of the statistical analysis on the experimental data with the help of a computer program (which uses the least square method as a regression technique). Fig. 8 shows a comparison of the measured heat transfer coefficient from experiments and the calculated heat transfer coefficient by Eq. (2). The suggested empirical correlation predicts the experimental data within ±15% error band, with some exceptions from the fitted data of Eq. (2). This is because of the complex heat transfer mechanisms in annuli [6,7]. The scatter bound is much wider at the annuli with closed bottoms comparing to the open bottoms since the boiling mechanism for the closed case is much more complex than the annuli with open bottoms. The flow in an annulus with open bottoms is steady while the flow in an annulus with closed bottoms are pulsating. Active boiling initiation is expected even at the lower heat fluxes for the closed bottoms [6]. The scatter of the present data is of similar size to that found in other existing pool boiling data. As noted by

Table 2
Results of curve fitting for h_b versus q'' data

Parameter	Parametric value	Standard deviation
C_1	0.77145	0.05947
C_2	0.68937	0.01678
C_3	0.02691	0.01811
C_4	−0.06455	0.01075

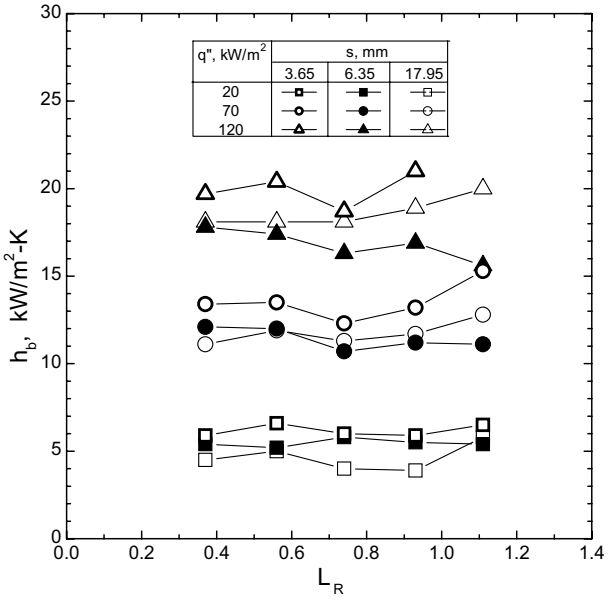

Fig. 7. Plots of h_b versus $L_R(=L_o/L)$ as q'' changes.

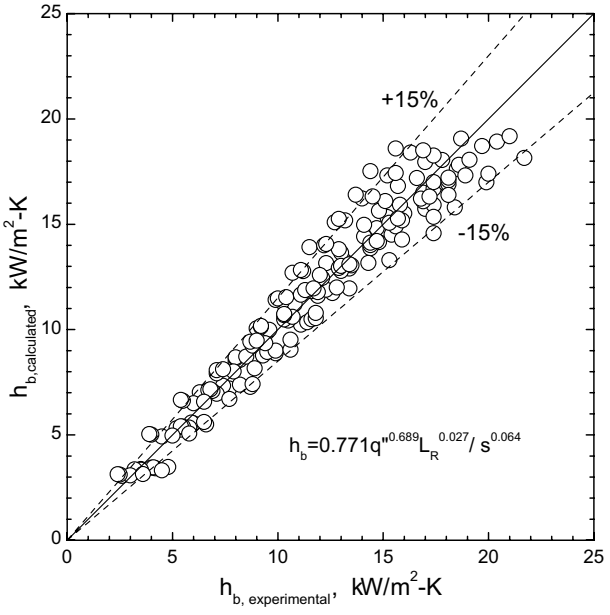

Fig. 8. Comparison of calculated heat transfer coefficients to the coefficients from experiments.

Cornwell and Houston [11], there seems to be some inherent randomness in pool boiling due to the uncertainties associated with nucleation site density, physical conditions of the tube surface and others. This fact precludes greater accuracy of both theoretical and empirical correlations for heat transfer coefficients in nucleate boiling.

4. Conclusions

To identify effects of the outer tube length on pool boiling heat transfer in a vertical annulus with closed bottoms, a heated tube of 19.1 mm diameter and water at atmospheric pressure have been studied experimentally. The combinations of five tube lengths (0.2–0.6 m) and three gap sizes (3.65, 6.35, and 17.95 mm) are investigated. Through the analyses on the results, following conclusions have been obtained:

1. The existence of the outer tube increases the heat transfer coefficient regardless of the gap size and the length.
2. The change in the outer tube length results in much variation in heat transfer coefficients. The improvement in heat transfer is more clearly observed, as the gap size gets small (for the case, 3.65 and 6.35 mm) because of the much frequent bubble coalescence and stronger pulsating movement.
3. As the outer tube length is shorter than the heated tube the deterioration point of the heat transfer coefficients gets moved up to the higher heat fluxes and the possibility of the CHF creation can be prevented.
4. To identify effects of the outer tube length on heat transfer an empirical correlation has been suggested in terms of the gap size, the tube ratio, and the heat flux. The correlation predicts reasonably the measured data within $\pm 15\%$ scattering band.

Acknowledgement

The academic research support program from Andong National University supported this work.

References

[1] M. Shoji, Studies of boiling chaos: a review, Int. J. Heat Mass Transfer 47 (2004) 1105–1128.
[2] M.H. Chun, M.G. Kang, Effects of heat exchanger tube parameters on nucleate pool boiling heat transfer, ASME J. Heat Transfer 120 (1998) 468–476.
[3] Y.J. Chung, S.H. Yang, H.C. Kim, S.Q. Zee, Thermal hydraulic calculation n a passive residual heat removal system of the SMART-P plant for forced and natural convection conditions, Nucl. Eng. Des. 232 (2004) 277–288.
[4] S.C. Yao, Y. Chang, Pool boiling heat transfer in a confined space, Int. J. Heat Mass Transfer 26 (1983) 841–848.
[5] Y.H. Hung, S.C. Yao, Pool boiling heat transfer in narrow horizontal annular crevices, ASME J. Heat Transfer 107 (1985) 656–662.
[6] M.G. Kang, Pool boiling heat transfer in vertical annular crevices, Int. J. Heat Mass Transfer 45 (15) (2002) 3245–3249.
[7] M.G. Kang, Y.H. Han, Effects of annular crevices on pool boiling heat transfer, Nucl. Eng. Des. 213 (2002) 259–271.
[8] M.G. Kang, Effects of outer tube length on saturated pool boiling heat transfer in a vertical annulus with closed bottom, Int. J. Heat Mass Transfer 85 (13) (2005) 2795–2800.
[9] Y. Fujita, H. Ohta, S. Uchida, K. Nishikawa, Nucleate boiling heat transfer and critical heat flux in narrow space between rectangular spaces, Int. J. Heat Mass Transfer 31 (1988) 229–239.
[10] J. Bonjour, M. Lallemand, Flow patterns during boiling in a narrow space between two vertical surfaces, Int. J. Multiphase Flow 24 (1998) 947–960.
[11] K. Cornwell, S.D. Houston, Nucleate pool boiling on horizontal tubes: a convection-based correlation, Int. J. Heat Mass Transfer 37 (1) (1994) 303–309.